Solar Energy 190 (2019) 608–616

Contents lists available at ScienceDirect

Solar Energy

journal homepage: www.elsevier.com/locate/solener

Numerical studies of thermal comfort for semi-transparent building integrated photovoltaic (BIPV)-vacuum glazing system

Aritra Ghosh[a,*], Nabin Sarmah[b], Senthilarasu Sundaram[a], Tapas K. Mallick[a]

[a] Environmental and Sustainability Institute, University of Exeter, Penryn, Cornwall TR10 9FE, UK
[b] Department of Energy, Tezpur University, Tezpur, Assam Pin-784028, India

ARTICLE INFO

Keywords:
BIPV
Glazing
Vacuum
Thermal comfort
PVM
Temperate

ABSTRACT

Building integrated photovoltaic (BIPV)-vacuum system is promising for advanced window application due to its ability to reduce heat transfer, control over admitted solar heat and generates environmentally benign electricity. In this work, numerically thermal comfort for an unfurnished room comprising of BIPV-vacuum glazing was evaluated for the United Kingdom (UK) climate. Required parameters to determine thermal comfort, one-dimensional heat transfer model was developed and validated for BIPV-vacuum glazing and results were compared with BIPV-double-pane glazing system. PV cell temperature difference between these two different types of glazing was 24 °C. For the UK climate, BIPV-vacuum glazing offered 26% higher room temperature at clear sunny day compared to BIPV-double system. BIPV–vacuum glazing system provided soothing or comfortable thermal comfort during mid-day period for a clear sunny day at temperate climate. In a combined BIPV-vacuum glazing, it was also predicted that vacuum glass facing external ambient is suitable for the UK climate whilst vacuum glass facing internal room ambient is applicable for Indian climate.

1. Introduction

Energy consumption has been increased extensively due to the recent development of industry and agriculture. The majority of this energy is generated from fossil fuel, which causes adverse environmental pollution. To address this detrimental issue, renewable energy generation by using onsite benign power generation from photovoltaic (PV) installed in a building is one of the potential approaches which reduces the necessity of large land requirement and the transmission power losses. Thus for urban buildings, building-integrated PV (BIPV) is one of the best choices (Biyik et al., 2017; Peng et al., 2011; Shukla et al., 2018) because of its aesthetic appearance and ability to offset the initial cost.

BIPV in a building replaces traditional wall (Taffesse et al., 2016), roof (Ritzen et al., 2017) window by semi-transparent glazed window (Sun et al., 2018) or can be installed as large glazed façade for commercial building (Saretta et al., 2019; Shukla et al., 2018). Semi-transparent BIPV glazing limits entering solar heat gain, daylight and generates benign electricity while PV can be semi-transparent type (Lee and Ebong, 2017) or spaced type opaque (Karthick et al., 2018; Park et al., 2010) materials, sandwiched between two glass sheets as shown in Fig. 1. Investigated semi-transparent type PV materials for glazing application include 2nd generation thin-film amorphous silicon (Wang et al., 2017), cadmium telluride (Alrashidi et al., 2019; Sun et al., 2018), copper indium selenide and third or emerging perovskite (Cannavale et al., 2017; Ghosh et al., 2020), dye-sensitized (Ghosh et al., 2018a; Selvaraj et al., 2019), and organic (Chemisana et al., 2018) types. However, these semi-transparent PV materials suffer from low luminous transmittance, spectral distortion of transmitted incoming daylight into indoor space and low durability (Lee and Ebong, 2017) (Mehmood et al., 2017) (Jordan and Kurtz, 2013). First-generation crystalline silicon (c-Si) PV is still in research interest for BIPV application as it exhibits higher stability, persistent performance with the highest cell and module efficiency (Green et al., 2019). To eliminate the blocking of light due to the opaque nature of c-Si, spaced are created between PV cells (Park et al., 2010) on a transparent substrate (Traverse et al., 2017).

Currently, different investigated BIPV glazings include, double panes airflow semi-transparent PV glazing (Chow et al., 2007; Zhang et al., 2016), double panes thermally insulated PV glazing (Cuce et al., 2016; Young et al., 2014), and single-pane PV glazing (He et al., 2011). For airflow BIPV glazing, between external PV layer and internal glass panes, intermediate cavity allows flowing of cold air to reduce the cavity air temperature which enhances the thermal comfort for indoor and increases the power generation from PV (Peng et al., 2016, 2015; Wang et al., 2017). Airflow BIPV glazing types are suitable for new

* Corresponding author.
E-mail addresses: a.ghosh@exeter.ac.uk (A. Ghosh), t.k.mallick@exeter.ac.uk (T.K. Mallick).

https://doi.org/10.1016/j.solener.2019.08.049
Received 8 May 2019; Received in revised form 7 August 2019; Accepted 17 August 2019
Available online 28 August 2019

Nomenclature

A_g	area of glazing (m^2)
C_{air}	specific heat of air (kJ/kg K)
h_0	external heat transfer coefficient (W/m^2K)
I	incident radiation (W/m^2)
I_{cl}	thermal resistance of clothing ($m^{20}C/W$)
k_g	thermal conductivity of glass (W/m^2K)
L_g	thickness of glass (m)
$L_{polystyrene}$	thickness of polystyrene (m)
M	metabolic rate in (W/m^2) of the body surface area (W/m^2)
$M_{test\ cell}$	mass of the air inside test cell (kg)
$T_{ambient}$	ambient temperature (K)
T_{cl}	clothing surface temperature (K)
T_{pv}	temperature of PV cell (K)
T_{rm}	mean radiant temperature (K)
$T_{testcell}$	test cell temperature (K)
p	pillar spacing (m)
P_a	water vapour partial pressure (Pascal)
R_g	thermal resistance associated with glass (m^2K/W)
R_{pillar}	thermal resistance associated with pillar (m^2K/W)
R_0	thermal resistance associated with external heat flow (m^2K/W)
R_r	thermal resistance associated with radiate heat flow (m^2K/W)
U1	total heat transfer coefficient from PV module to ambient through glass cover (W/m^2K)
U2	total heat transfer coefficient from PV module and vacuum glazing to test cell through glass (W/m^2K)
U3	total heat transfer coefficient from lower glass to test cell (W/m^2K)
V_{air}	relative air velocity (m/s)
W	effective mechanical power, equal to zero for most effectives
τ	transmissivity
β	packing factor
β_0	temperature coefficient of PV (/°C)
ε	emittance of a surface
σ	Stefan–Boltzmann constant ($5.67 \times 10^{-8}\ W\ m^{-2}\ K^{-4}$)
h_c	convective heat transfer coefficient (W/m^2K)
f_{cl}	ratio of surface area of the body with clothes to the surface area of the body without clothes
1,2,3	represents number of glass

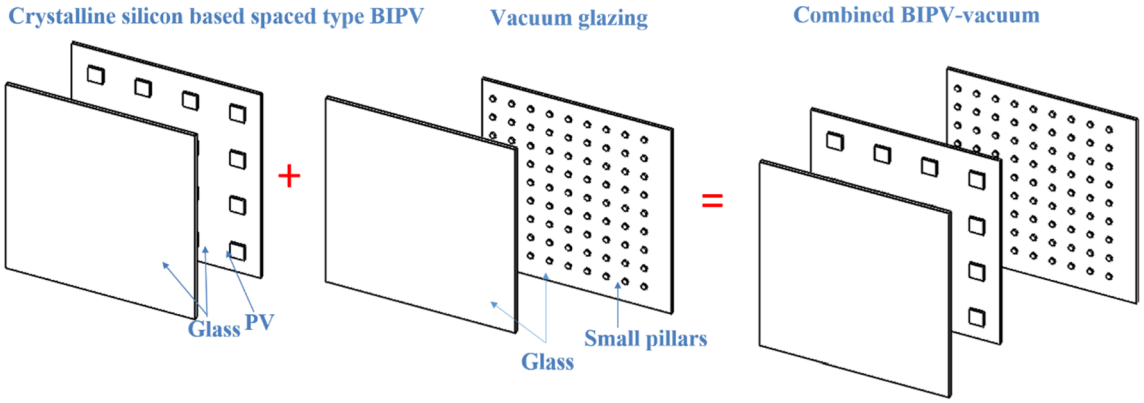

Fig. 1. Schematic of semi-transparent BIPV-vacuum glazing system.

buildings in a hot climate; however, they are intricate for retrofit building integration. For insulated type BIPV glazing, sealed air cavity remains between external PV glass and inner glass panes to reduce the thermal transmission and makes it suitable for cold climate (Young et al., 2014). Higher or lower thermal transmission is possible by varying the air cavity thickness of insulated BIPV systems. This double-glazing type BIPV is impeccable for retrofit and new buildings due to its simpler structure.

To render further low thermal transmission, integration of BIPV glazing with vacuum type glazing is possible (Huang et al., 2018; Qiu et al., 2019) (Ghosh et al., 2018b). Vacuum glazing consists of two sealed glass panes to maintain vacuum (< 0.1 Pa) between them, which offers lower heat transfer compared to double and single glazing (Ghosh et al., 2016). Alumina, stainless steel, or nickel-based alloy support pillars having a typical diameter of 0.25 mm and 0.1 mm in height, are positioned in a square array, separated by 20 mm between two glasses to counteract the external ambient pressure (Fang et al., 2014). Solder glass (Collins and Simko, 1998), indium alloy (Griffiths et al., 1998) and cerasolzer type CS186 (Memon et al., 2015) edge sealed vacuum glazing were fabricated at University of Sydney, University of Ulster, and Loughborough University respectively. Transparent pillars were also under investigation (Zhao et al., 2013) to eliminate the negligible optical obstacle. Thermal performance of vacuum glazing using simulation (Fang et al., 2009), indoor (Fang et al., 2006) and outdoor experimental (Ghosh et al., 2016) characterization showed that vacuum glazing is suitable for cold climate due to its low overall heat transfer coefficient. Optical (Ghosh et al., 2017) and daylighting (Ghosh et al., 2016) performance of vacuum glazing indicated that it transmits a similar amount of daylight to air-filled double glazing.

Combined BIPV-vacuum (as shown in Fig. 1) system concomitantly offers low overall heat transfer coefficient, control over admitted solar heat gain and penetrated daylight, and generates benevolent clean electricity (Ghosh and Norton, 2018) (Huang et al., 2018). A previous study using c-Si-based BIPV-vacuum system showed 0.8 W/m^2K overall heat transfer coefficient (Ghosh et al., 2018b). In another work, amorphous silicon PV based BIPV and vacuum combination reduced up to 81.63% of heat gain and 31.94% of heat loss in Hong Kong compared to the baseline window system (Huang et al., 2018; Qiu et al., 2019). External daylight passing through a-Si can distort the daylight spectrum, which may create indoor discomfort. Thus, to obtain colour comfort, a combined BIPV-vacuum system using spaced type c-Si was investigated to allow comfortable daylight through the space between two cells. Therefore, indoor daylight quality similar to external daylight is achievable using this spaced type semi-transparent BIPV-vacuum system (Ghosh et al., 2019).

For low energy building, thermal comfort is an essential parameter to be considered as it expresses human satisfaction for the varying thermal environment. Suitable thermal comfort allows a healthy

environment to work whilst inappropriate thermal comfort lowers work efficiency. Thermal comfort depends on various psychological, physiological and behavioural factors and varies with perception and expectation of individual building occupant (Eniolu et al., 2018; Shahzad et al., 2018; Thapa et al., 2018). Reported thermal comfort evaluation work using PV glazed system is rare. He et al. (2011) investigated thermal comfort for a-Si PV windows in East China. Best thermal comfort was achieved when a single glazing was employed. Thus, evaluation of thermal comfort to minimize carbon footprint from low energy new or retrofit building integrated with BIPV-vacuum glazing is paramount.

In this work, for the first time, thermal comfort analysis of the c-Si-based BIPV-vacuum glazing system was evaluated at temperate climate (UK) using predicted mean vote (PVM) analysis and results were compared with BIPV double glazed window system. Room temperatures for both type glazing were investigated using a one-dimensional heat transfer model, which were validated from our previous experimental work (Ghosh et al., 2018b).

2. System description and experiment

Semi-transparent BIPV-vacuum glazing was fabricated using one vacuum glazing, one multi-crystalline PV cell, and one single glass. This NSG SPACIA vacuum glazing and Pilkington single k glass had a dimension of 0.35 m × 0.2 m while the solar cell was 0.155 m × 0.155 m. In this structure, the PV cell covered 32% whereas 68% area was non-covered by PV. One glass-PV-glass BIPV double glazing was also fabricated to compare the performance of BIPV -vacuum. Details of these two systems are mentioned in Table1. A test cell dimension of 0.37 m × 0.22 m × 0.26 m made of 10 cm thick polystyrene was fabricated to perform indoor characterization. The ratio of glazing and test cell was 1:1. The indoor characterisation was performed using continuous indoor sun simulator exposure. This simulator is an AAA type, and its spectrum matches with a solar spectrum between 250 nm and 3000 nm. Five thermocouples were employed to measure external and internal glass surface, test cell ambient and indoor laboratory ambient and PV cell temperature. Pico data logger recorded 5 min interval temperature data. The schematic of the experimental set up is shown in Fig. 2.

3. Theory and methodology

3.1. Thermal analysis of BIPV-vacuum and BIPV double glazing

Structure of BIPV-vacuum glazing placed in a test cell is shown in Fig. 3(a) and equivalent thermal resistance networks are shown in Fig. 3(b) and (c).

Energy balance equations were written using the following assumptions-:(Gaur et al., 2016).

- Negligible ohmic losses,
- System was in quasi-steady state,
- One-dimensional heat transfer was considered to be dominant from the interior to the exterior through the system and surface of the PV module was at a uniform temperature,
- The test cell was thermally insulated and made by homogeneous highly insulating material.

Energy balance for semi-transparent BIPV –vacuum glazing can be represented by Eq. (1)

$$\tau_g \alpha_g \beta I A_g = U_1 (T_{pv} - T_{ambient}) A_g + U_2 (T_{pv} - T_{testcell}) A_g + \eta_{pv} I A_g \quad (1)$$

From simplification of Eq. (1), PV cell temperature Eq. (2) is obtained

$$T_{pv} = \left(\frac{\tau_g \alpha_g \beta I - \eta_{pv} I + U_1 T_a + U_2 T_{testcell}}{U_1 + U_2} \right) \quad (2)$$

where

$$U_1 = (R_{g3} + R_0)^{-1}$$

$$U_2 = \left[\frac{R_{pillar}(R_{g2} + R_r)}{R_{pillar} + R_{g2} + R_r} + R_{g3} \right]^{-1}$$

$$R_g = \frac{L_g}{k_g},\ R_0 = \frac{1}{h_0},\ R_{pillar} = \frac{p^2}{2k_g a},\ R_r = (4\sigma\varepsilon T^3)^{-1}$$

Energy balance for test cell can be represented by Eq. (3)

$$\tau_g^2 \alpha_g (1 - \beta) I A_g = M_{testcell} C_{air} \frac{dT_{testcell}}{dt} - U_2 A_g (T_{pv} - T_{testcell}) + U_3 (T_{testcell} - T_{ambient}) A_g \quad (3)$$

where

$$U_3 = (R_i + R_{testcell})^{-1}$$

$$R_i = \frac{1}{h_i},\ R_{testcell} = \frac{L_{polystyrene}}{k_{polystyrene}}$$

Rearranging Eq. (3), following Eq. (4) can be obtained

$$\frac{dT_{testcell}}{dt} + T_{testcell} \left[\frac{U_4 A_g (U_2 + U_3)}{M_{testcell} C_{air} U_4} \right] = \left[\frac{U_4 \tau_g^2 \alpha_g (1 - \beta) I A_g + U_4 U_3 A_g T_{ambient} + U_2 A_g \tau_g \alpha_g \beta I + U_2 A_g U_1 T_{ambient} - U_2 A_g \eta_{pv} I}{M_{testcell} C_{air} U_4} \right] \quad (4)$$

Eq. (4) can be written in simplified form as Eq. (5)

$$\frac{dT_{testcell}}{dt} + T_{testcell} A = B \quad (5)$$

where $A = \left[\frac{U_4 A_g (U_2 + U_3)}{M_{testcell} C_{air} U_4} \right]$ and $B = \frac{U_4 \tau_g^2 \alpha_g (1 - \beta) I A_g + U_4 U_3 A_g T_a + U_2 A_g \tau_g \alpha_g \beta I + U_2 A_g U_1 T_a - U_2 A_g \eta_{pv} I}{M_{testcell} C_{air} U_4}$

Using initial boundary condition at time t = 0 and $T_{test\ cell} = T_{testcell,i}$; $T_{testcell}$ can be found by integration

$$T_{testcell} = \frac{B}{A} [1 - \exp(-At)] + T_{tescell,i} \exp(-At) \quad (6)$$

Temperature dependent PV efficiency (Skoplaki and Palyvos, 2009) of PV cell can be found

$$\eta_{pv} = \eta_0 [1 - \beta_0 (T_{pv} - T_{testcell,i})] \quad (7)$$

Substituting T_{pv}, A and B, efficiency is given by equation (8)

$$\eta_{pv} = \frac{\eta_0 [X - Y \{1 - \exp(-At)\}] + \left(\frac{\eta_0 \beta_0 U_2}{U_4} \right) T_{testcell,i} \exp(-At)}{Z} \quad (8)$$

where

$$X = \left[1 - \frac{\beta_0 (\tau_g \beta I + U_1 T_a)}{U_4} + \beta_0 T_{ri} \right]$$

$$Y = \frac{\eta_0 \beta_0 U_2}{U_4 [U_4 (U_2 + U_3) - U_2^2]} [U_4 \tau_g^2 (1 - \beta) I + U_4 U_3 T_a + U_2 \tau_g \beta I + U_2 U_1 T_a]$$

$$Z = 1 - \frac{\eta_0 \beta_0 I}{U_4} - \frac{U_2^2 I \beta_0 \eta_0 \{1 - \exp(-At)\}}{U_4 [U_4 (U_2 + U_3) - U_2^2]}$$

For BIPV-double glazing equivalent thermal network is shown in Fig. 4.

Table 1
Details of investigated systems.

Types	Thickness
BIPV-Vacuum glazing	12 mm
BIPV-double glazing	8 mm

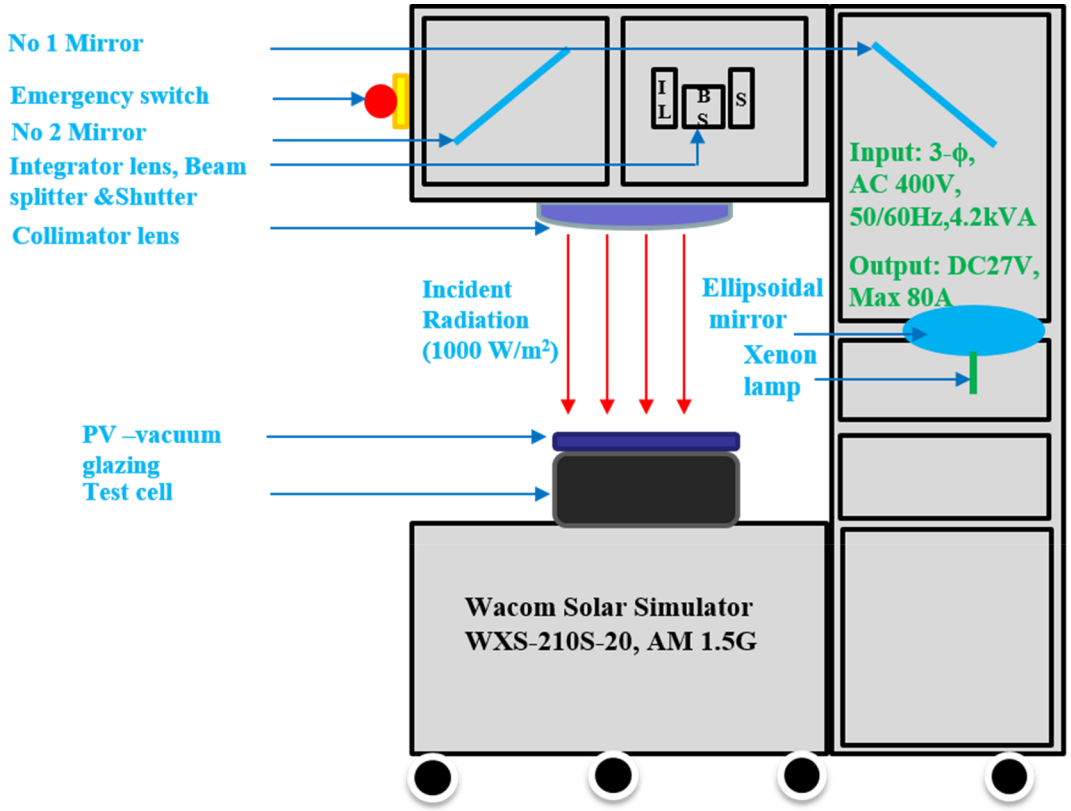

Fig. 2. Schematic of indoor experimental set up using test cell and indoor simulator and combined semi-transparent BIPV-vacuum glazing system.

BIPV-double glazing consists of two glass panes. Except for U2 all other components are similar to BIPV- vacuum glazing. Thus, the equation for PV temperature (T_{pv}), test cell temperature ($T_{testcell}$), and PV cell efficiency (η_{pv}) of PV double glazing will be similar to BIPV-vacuum glazing, and only modification is required for U2.

U2 for BIPV double glazing is given by

$$U_2 = [R_{g2}]^{-1} \tag{9}$$

To compare theoretical and experimental result, correlation coefficient (r) and root mean square percent deviation (e) were evaluated by using following equation

$$r = \frac{N\sum X_j Y_j - (\sum X_j)(\sum Y_j)}{\left[\sqrt{N\sum X_j^2 - (\sum X_j)^2}\right]\left[\sqrt{N\sum Y_j^2 - (\sum Y_j)^2}\right]} \tag{10}$$

$$e = \sqrt{\frac{\sum\left(\frac{X_j - Y_j}{X_j}\right)^2}{N}} \tag{11}$$

3.2. Thermal comfort analysis

Predicted mean vote (PMV) and predicted percentage dissatisfied

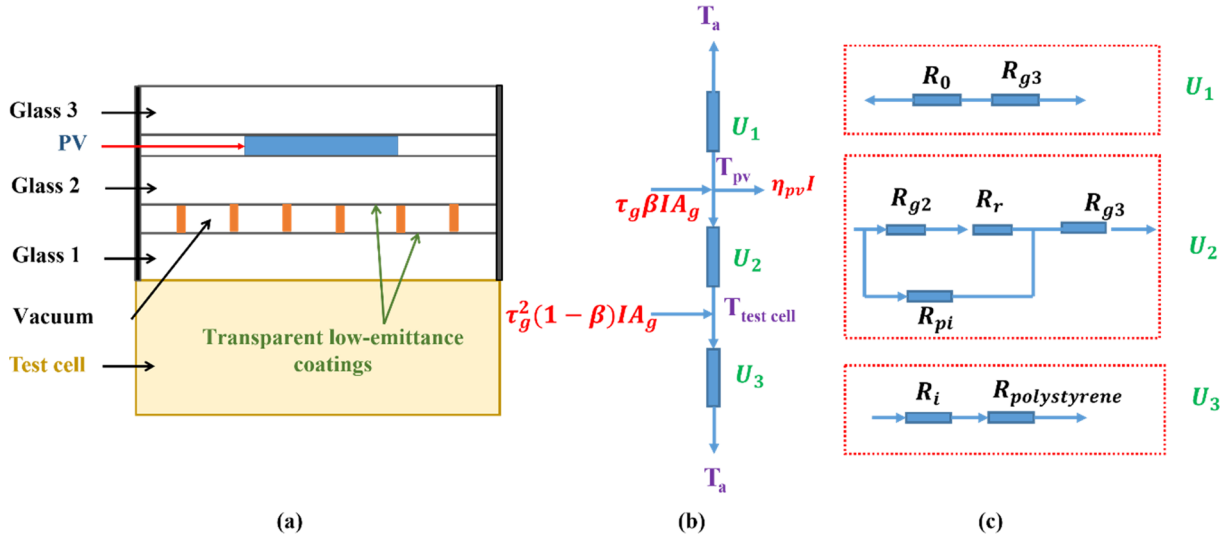

Fig. 3. (a) Structure of BIPV-vacuum glazing attached in the top of the test cell, (b) Thermal diagram of the BIPV-vacuum glazing, (c) Detail thermal diagram for U1, U2, U3.

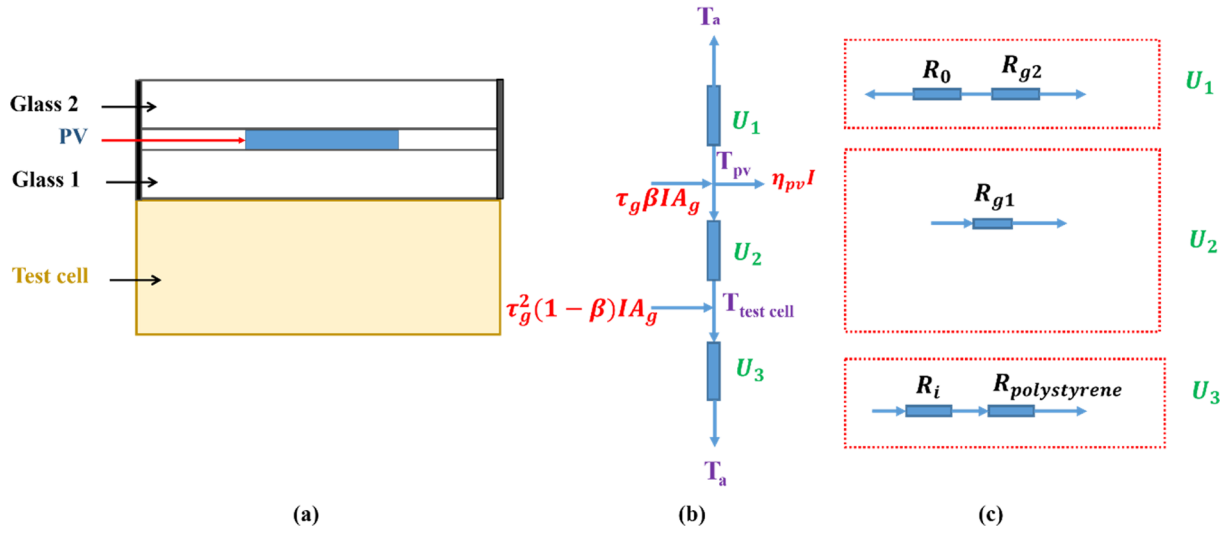

Fig. 4. (a) Structure of BIPV-double glazing attached in the top of the test cell, (b) Thermal diagram of the BIPV-double glazing, (c) Detail thermal diagram for U1, U2, U3.

Table 2
Thermal sensation vote or thermal comfort level for indoor temperature.

Sensation	Scale value
Hot	+3
Warm	+2
Slightly warm	+1
Neutral	0
Slightly cool	−1
Cool	−2
Cold	−3

Table 3
Assumption for thermal comfort evaluation.

Detail of input parameter	Details of dimension and values
Room Dimension	4 m × 4 m × 3 m; The person is seated 1 m away from the window which occupies entire external facade (4 m × 3 m). Window means here only glazing without frame.
Clothing insulation (I_{cl})	0.5 Summer 1 winter
Metabolic rate (M)	1.2 summer 1.0 winter Relaxed seated person is 1
Solar absorptance of a person	0.6
Emittance of human body	0.97
Projected area factor of person	0.3
Water vapour pressure (Pa)	1587 Pascal (kg/m^2s^2)

(PPD) are the two used methods to assess thermal comfort (ISO, 2009; Pourshaghaghy and Omidvari, 2012; Singh et al., 2008; Wang et al., 2018). This method includes two human factors such as metabolic rate and clothing insulation and four environmental parameters such as air temperature, relative humidity, air velocity, and mean radiant temperature. External diurnal variation of solar radiation and ambient temperature creates a temperature difference between BIPV-vacuum glazing and interior walls, which leads to asymmetrical thermal radiation and a variety of thermal comfort level. Thus, the PMV index is employed to evaluate the indoor thermal comfort level, which is expressed by Eq. (12), and PPD is given by Eq. (16).

$$PMV = (0.303e^{-0.036M} + 0.028) \times \begin{Bmatrix} (M-W) - 3.05\times10^{-3}\times[5733 - 6.99(M-W) - P_a] \\ -(0.42)\times[(M-W) - 58.15] - 1.7\times10^{-5}M(5867 - P_a) \\ -0.0014M(34 - T_{ambient}) \\ -(3.96)\times10^{-8}\times f_{cl}\times[(T_{cl}+273)^4 - (T_{rm}+273)^4] \\ -f_{cl}h_c(T_{cl} - T_{ambient}) \end{Bmatrix} \quad (12)$$

where, clothing temperature (T_{cl}), heat transfer coefficient (h_c), ratio of surface area of the body with clothes to the surface area of the body without clothes (f_{cl}) are given by Eqs. (13)–(15) respectively.

$$T_{cl} = 35.7 - 0.028(M-W) - \{3.96\times10^{-8}f_{cl}\times[(T_{cl}+273)^4 - (T_{rm}+273)^4] + f_{cl}h_c(T_{cl} - T_{ambient})\} \quad (13)$$

$$h_c = \begin{bmatrix} 2.38(T_{cl} - T_a)^{0.25} for\ 2.38\times|T_{cl} - T_{ambient}|^{0.25} > 12.1\sqrt{V_{air}} \\ 12.1\sqrt{V_{ar}}\ for\ 2.38\times|T_{cl} - T_{a,bient}|^{0.25} < 12.1\sqrt{V_{air}} \end{bmatrix} \quad (14)$$

$$f_{cl} = \begin{Bmatrix} 1.00 + 1.290\times I_{cl}\ for\ I_{cl} \leqslant 0.078\ m^2K/W \\ 1.05 + 0.645\times I_{cl}\ for\ I_{cl} > 0.078\ m^2K/W \end{Bmatrix} \quad (15)$$

$$PPD = 100 - 95\times\exp(-0.03353\times PMV^4 - 0.2179\times PMV^2) \quad (16)$$

The appropriate range for thermal comfort is $-0.5 < PMV < 0.5$ in which 90% of people have comfort sense. More explanations on thermal comfort and its calculations are found in (ISO, 2009). The thermal sensation votes (TSV) for the indoor temperature were received in ASHRAE 7-point scale as listed in Table 2. Table 3 shows the assumed parameters to evaluate thermal comfort (ASHRAE-55, 2010; ISO, 2009).

4. Results and discussion

4.1. Validation of thermal analysis

To validate the PV cell temperature, efficiency and room temperature model, the experiment was performed at indoor condition for 120 min under 1000 W/m^2 continuous exposure from constant indoor solar spectrum. The theoretically calculated and experimentally measured test cell indoor temperature for BIPV-vacuum glazing is shown in Fig. 5a. After 120 min of exposure, the test cell room temperature of BIPV-vacuum glazing was close to 50 °C. Test cell temperature increased at a rate of 12 °C/h. The values of correlation coefficient (r) and

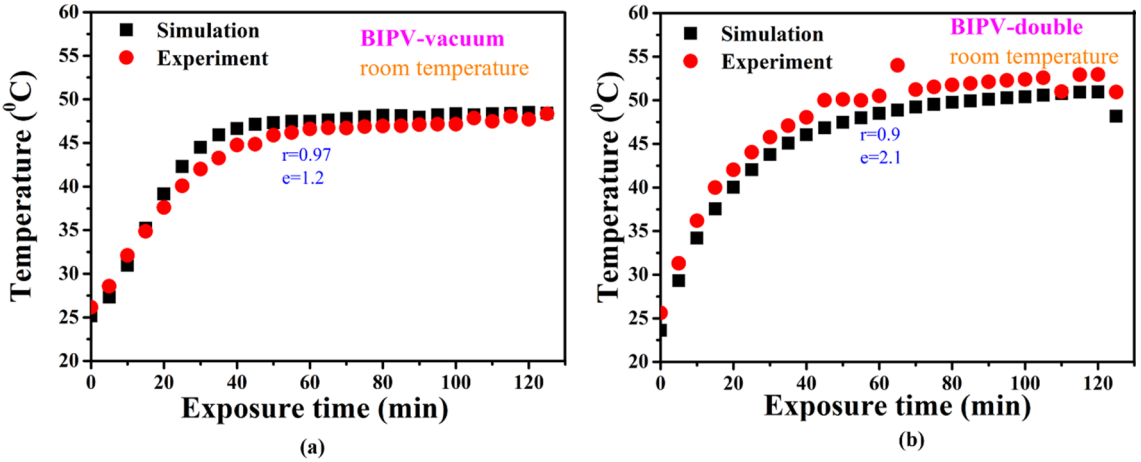

Fig. 5. Variation of theoretically (simulated) calculated and experimentally measured test cell indoor temperature of (a) BIPV-vacuum glazing system and (b) BIPV-double glazing system.

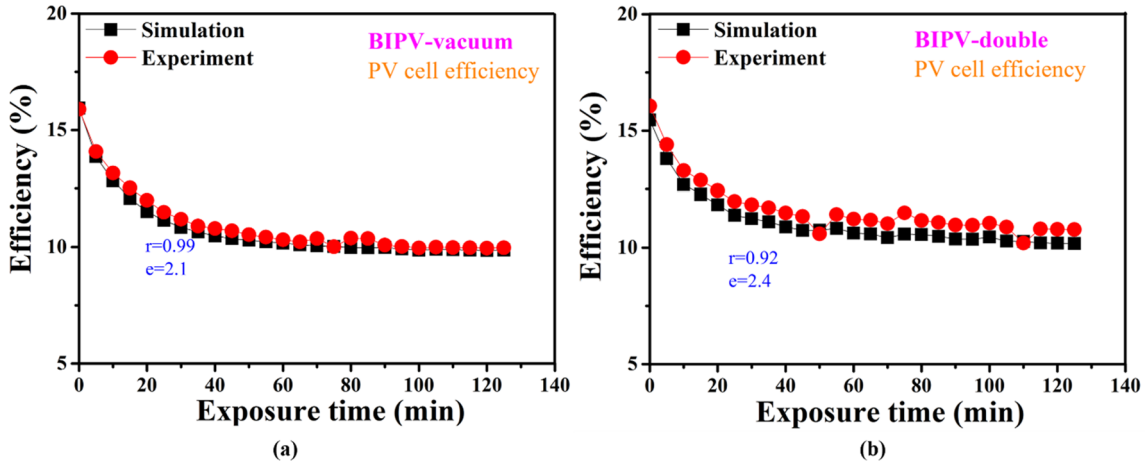

Fig. 6. Variation of PV cell efficiency of theoretically calculated and experimentally measured data of (a) BIPV-vacuum glazing system and (b) BIPV-double glazing system.

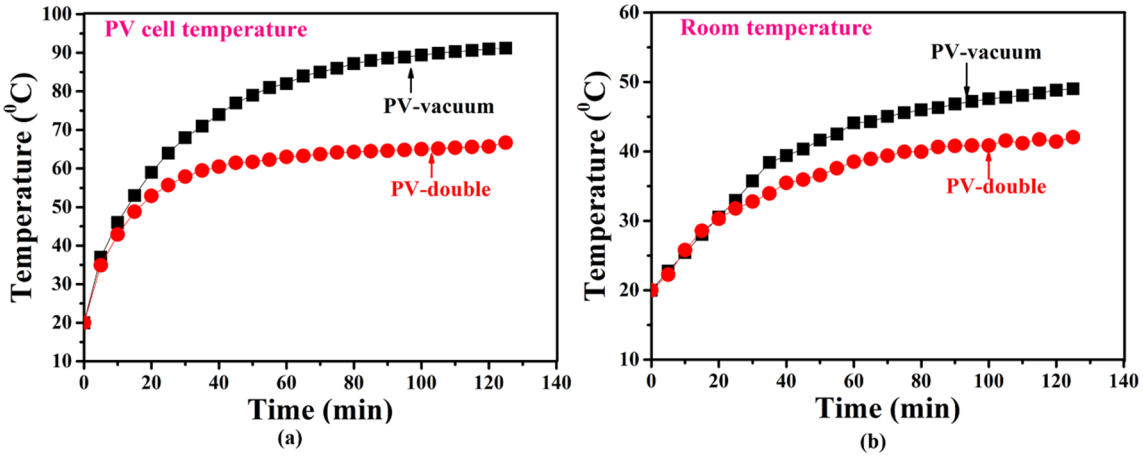

Fig. 7. Calculated PV cell temperature and test cell temperature for (a) BIPV-vacuum and (b) BIPV-double glazing.

root mean square percent deviation (e) was calculated using Eqs. (10) and (11) respectively and have also been shown in the Fig. 5. The maximum deviation of temperature was found to be 3.8 and the value of r was 1.8. It can be inferred that theoretical and experimental temperature closely matches with each other. The PV cell efficiency for BIPV-vacuum system was indicated in Fig. 6a. From experimentally measured data, the PV cell efficiency decreased from 15% to 8% for BIPV-vacuum glazing and 15% to 10.5% for BIPV-double glazing. The decrement was due to the higher cell temperature at higher exposure time. Theoretically, the efficiency was calculated using Eq. (8). The maximum deviation between theoretical and experimentally measured efficiency was 2.2 which indicates that this theoretical model is a

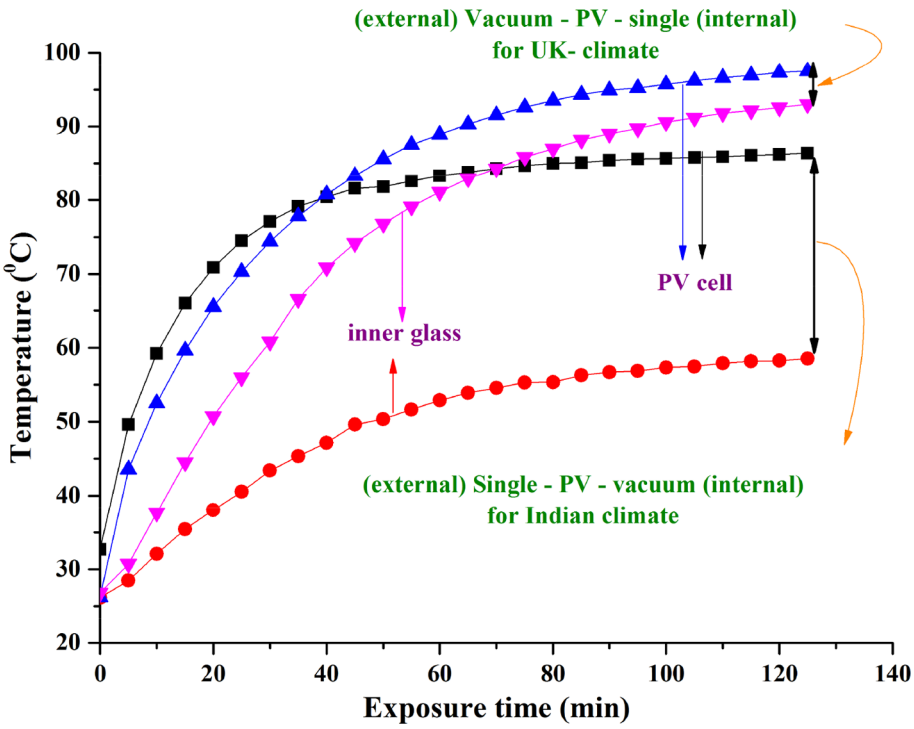

Fig. 8. Inner glass and PV cell temperature for Single-PV-vacuum (SPV) and Vacuum-PV- single (VPS) type combined BIPV-vacuum glazing system for India and UK climate respectively.

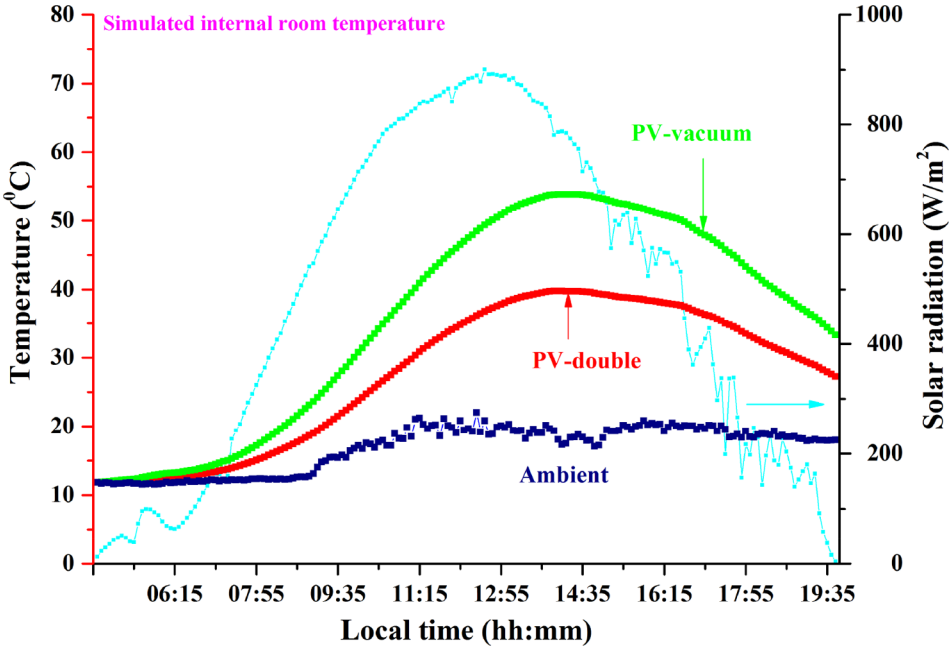

Fig. 9. Internal room temperature for BIPV-vacuum and BIPV-double glazing.

promising method to predict the efficiency accurately from the measured incident light and ambient temperature parameters. Measured solar radiation and ambient temperature for Exeter climate were given as input in the numerical equation to predict the test room temperature and PV cell temperature of both BIPV-vacuum and BIPV –double glazing systems as shown in Fig. 7. PV cell temperature for two different type of glazing showed 24 °C temperature difference which was due to vacuum glazing's excellent heat insulation property. Vacuum system restricts radiative heat flow due to the presence of low emission coating, reduces conductive and convective heat flow due to the presence of vacuum space between two glasses. Initially, in Fig. 7b, the room temperature of BIPV-vacuum glazing increased equally with BIPV-double glazing. However, due to the heat retention property of vacuum glazing, the heat was blocked in the test room, which enhanced the temperature for both PV cell and test cell.

For vertical plane glazing, from external ambient to internal room ambient, single –PV –vacuum (SPV) glazing or vacuum-PV-single (VPS) glazing are the two possible types of BIPV-vacuum system. These two structures are suitable for two different climatic zones. At higher temperatures, PV (c-Si) emits thermal radiation (Riverola et al., 2018) and

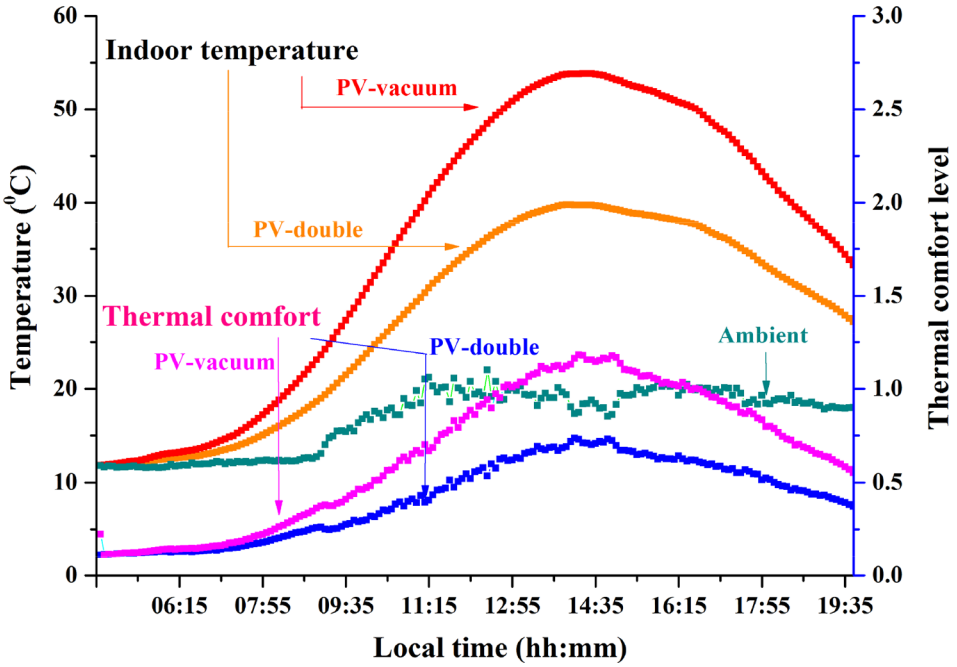

Fig. 10. Thermal comfort for BIPV-double glazing and BIPV -vacuum glazing for a typical clear sunny day at Exeter Penryn climate.

vacuum glazing has low emission coating which restricts to pass the thermal radiation (Fang et al., 2007). Thus, for Indian context where the climate is hot most of the time, SPV structure is potential. In reverse, VPS is suitable for the UK climate as emitted thermal radiation from PV restricted by vacuum glazing, thus cannot flow outside, as shown in Fig. 8. The temperature difference between the PV cell and inner glass for SPV was 28 °C while the temperature difference was 5 °C for VPS structure.

The internal room temperature is shown in Fig. 9 for an interior while room and glazing (1 m^2 glazed façade) has a 1:1 ratio. Ambient temperature and solar radiation were measured at the roof of ESI building, the University of Exeter, Penryn (50.16° N, −5.10° E) campus. At a mid-day period, 26% enhanced room temperature was achieved for the BIPV-vacuum system. These temperatures were predicted by using Eq. (6). Higher indoor temperature was obtained from BIPV-vacuum system due to vacuum glazing's heat retention property, which makes this system suitable for cold climate (Ghosh et al., 2016).

4.2. Thermal comfort

Fig. 10 shows the diurnal thermal comfort level for indoor while BIPV-double and BIPV-vacuum glazing were applied for a room, as mentioned in Table 3, Section 3.2. PVM was calculated using Eq. (12). Thermal comfort was calculated for a clear sunny day at Exeter climate. BIPV-vacuum glazing offered an allowable level of thermal comfort for Exeter climate in the morning time. Higher comfort level was achieved during the mid-day period for BIPV-vacuum glazing. At 1:00 pm, indoor temperature for BIPV-vacuum glazing was 25% higher than that of BIPV-double glazing, which produced 39% enhanced thermal comfort for temperate climate location. Variation of thermal comfort between BIPV–vacuum and BIPV double was higher at mid-day period and lower at early morning and afternoon time because of the direct influence of diurnal nature of incident solar radiation.

5. Conclusions

BIPV-vacuum combined glazing system possesses a low overall heat transfer coefficient, low solar heat gain and onsite benign electricity. In this work, thermal comfort using a novel BIPV-vacuum system was calculated for the temperate UK climate. Using measured solar radiation and ambient temperature and calculated indoor room temperature for a 1 m^2 BIPV-vacuum glazed system was employed to investigate the thermal comfort. Results were compared with a similar dimension of double glazed BIPV system. BIPV -vacuum system enhanced 39% of thermal comfort compared to BIPV-double glazing system for temperate climate location. Required room temperature for both glazings was calculated using a one-dimensional heat transfer model. Analytical expressions of electrical and thermal parameters for this BIPV-vacuum system were validated using an indoor experiment at the University of Exeter, Penryn, UK. A good agreement between the theoretical and experimental results was observed. It was also observed that the BIPV-vacuum structure could be (external ambient) single –PV-vacuum (internal room ambient) or (external room ambient) vacuum-PV-single (external room ambient) type. However, for UK climate vacuum-PV-single was found to be the best option.

Acknowledgement

This work has been conducted as part of the research project 'Joint UK-India Clean Energy Centre (JUICE)' which is funded by the RCUK's Energy Programme (contract no: EP/P003605/1). The projects funders were not directly involved in the writing of this article. This work was also supported partially by EPSRC-IAA grant achieved by Dr Aritra Ghosh. The research work has been carried out jointly at the Environmental and Sustainability Institute, University of Exeter, UK and Department of Energy, Tezpur University, India. In support of open access research, all underlying article materials (data, models) can be accessed upon request via email to the corresponding author.

References

Alrashidi, H., Ghosh, A., Issa, W., Sellami, N., Mallick, T.K., Sundaram, S., 2019. Evaluation of solar factor using spectral analysis for CdTe photovoltaic glazing. Mater. Lett. 237, 332–335. https://doi.org/10.1016/j.matlet.2018.11.128.

ASHRAE-55, 2010. Ashrae_Standard_55_2013_Thermal.Pdf.

Biyik, E., Araz, M., Hepbasli, A., Shahrestani, M., Yao, R., Shao, L., Essah, E., Oliveira, A.C., del Caño, T., Rico, E., Lechón, J.L., Andrade, L., Mendes, A., Atlı, Y.B., 2017. A key review of building integrated photovoltaic (BIPV) systems. Eng. Sci. Technol. an Int. J. 20, 833–858. https://doi.org/10.1016/j.jestch.2017.01.009.

Cannavale, A., Hörantner, M., Eperon, G.E., Snaith, H.J., Fiorito, F., Ayr, U., Martellotta,

F., 2017. Building integration of semitransparent perovskite-based solar cells: energy performance and visual comfort assessment. Appl. Energy 194, 94–107. https://doi.org/10.1016/j.apenergy.2017.03.011.
Chemisana, D., Moreno, A., Polo, M., Aranda, C., Riverola, A., Ortega, E., Lamnatou, C., Domènech, A., Blanco, G., Cot, A., 2018. Performance and stability of semi-transparent OPVs for building integration: a benchmarking analysis. Renew. Energy. https://doi.org/10.1016/j.renene.2018.03.073.
Chow, T.T., Fong, K.F., He, W., Lin, Z., Chan, A.L.S., 2007. Performance evaluation of a PV ventilated window applying to office building of Hong Kong. Energy Build. 39, 643–650. https://doi.org/10.1016/j.enbuild.2006.09.014.
Collins, R.E., Simko, T.M., 1998. Current status of the science and technology of vacuum glazing. Sol. Energy 62, 189–213. https://doi.org/10.1016/S0038-092X(98)00007-3.
Cuce, E., Cuce, P.M., Young, C.H., 2016. Energy saving potential of heat insulation solar glass: key results from laboratory and in-situ testing. Energy 97, 369–380. https://doi.org/10.1016/j.energy.2015.12.134.
Eniolu, T., Lau, K.K., Ren, C., Ng, E., 2018. Performance of Hong Kong's common trees species for outdoor temperature regulation, thermal comfort and energy saving. Build. Environ. 137, 157–170. https://doi.org/10.1016/j.buildenv.2018.04.012.
Fang, Y., Eames, P.C., Norton, B., Hyde, T.J., 2006. Experimental validation of a numerical model for heat transfer in vacuum glazing. Sol. Energy 80, 564–577. https://doi.org/10.1016/j.solener.2005.04.002.
Fang, Y., Eames, P.C., Norton, B., Hyde, T.J., Zhao, J., Wang, J., Huang, Y., 2007. Low emittance coatings and the thermal performance of vacuum glazing. Sol. Energy 81, 8–12. https://doi.org/10.1016/j.solener.2006.06.011.
Fang, Y., Hyde, T., Hewitt, N., Eames, P.C., Norton, B., 2009. Comparison of vacuum glazing thermal performance predicted using two- and three-dimensional models and their experimental validation. Sol. Energy Mater. Sol. Cells 93, 1492–1498. https://doi.org/10.1016/j.solmat.2009.03.025.
Fang, Y., Hyde, T.J., Arya, F., Hewitt, N., Eames, P.C., Norton, B., Miller, S., 2014. Indium alloy-sealed vacuum glazing development and context. Renew. Sustain. Energy Rev. 37, 480–501. https://doi.org/10.1016/j.rser.2014.05.029.
Gaur, A., Tiwari, G.N., Ménézo, C., Al-Helal, I.M., 2016. Numerical and experimental studies on a building integrated semi-transparent photovoltaic thermal (BiSPVT) system: model validation with a prototype test setup. Energy Convers. Manag. 129, 329–343. https://doi.org/10.1016/j.enconman.2016.10.017.
Ghosh, A., Bhandari, S., Sundaram, S., Mallick, T.K., 2020... Carbon counter electrode mesoscopic ambient processed & characterised perovskite for adaptive BIPV fenestration. Renew. Energy 145, 2151–2158. https://doi.org/10.1016/j.renene.2019.07.119.
Ghosh, A., Norton, B., 2018. Advances in switchable and highly insulating autonomous (self-powered) glazing systems for adaptive low energy buildings. Renew. Energy 126, 1003–1031. https://doi.org/10.1016/j.renene.2018.04.038.
Ghosh, A., Norton, B., Duffy, A., 2017. Effect of sky clearness index on transmission of evacuated (vacuum) glazing. Renew. Energy 105, 160–166. https://doi.org/10.1016/j.renene.2016.12.056.
Ghosh, A., Norton, B., Duffy, A., 2016. Measured thermal & daylight performance of an evacuated glazing using an outdoor test cell. Appl. Energy 177, 196–203. https://doi.org/10.1016/j.apenergy.2016.05.118.
Ghosh, A., Selvaraj, P., Sundaram, S., Mallick, T.K., 2018a. The colour rendering index and correlated colour temperature of dye-sensitized solar cell for adaptive glazing application. Sol. Energy 163, 537–544. https://doi.org/10.1016/j.solener.2018.02.021.
Ghosh, A., Sundaram, S., Mallick, T.K., 2019. Colour properties and glazing factors evaluation of multicrystalline based semi-transparent photovoltaic-vacuum glazing for BIPV application. Renew. Energy 131, 730–736. https://doi.org/10.1016/j.renene.2018.07.088.
Ghosh, A., Sundaram, S., Mallick, T.K., 2018b. Investigation of thermal and electrical performances of a combined semi- transparent PV-vacuum glazing. Appl. Energy 228, 1591–1600. https://doi.org/10.1016/j.apenergy.2018.07.040.
Green, M.A., Hishikawa, Y., Dunlop, E.D., Levi, D.H., Hohl-Ebinger, J., Yoshita, M., Ho-Baillie, A.W.Y., 2019. Solar cell efficiency tables (version 53). Prog. Photovolt. Res. Appl. 27, 3–12. https://doi.org/10.1002/pip.3102.
Griffiths, P.W., Di Leo, M., Cartwright, P., Eames, P.C., Yianoulis, P., Leftheriotis, G., Norton, B., 1998. Fabrication of evacuated glazing at low temperature. Sol. Energy 63, 243–249. https://doi.org/10.1016/S0038-092X(98)00019-X.
He, W., Zhang, Y.X., Sun, W., Hou, J.X., Jiang, Q.Y., Ji, J., 2011. Experimental and numerical investigation on the performance of amorphous silicon photovoltaics window in East China. Build. Environ. 46, 363–369. https://doi.org/10.1016/j.buildenv.2010.07.030.
Huang, J., Chen, X., Yang, H., Zhang, W., 2018. Numerical investigation of a novel vacuum photovoltaic curtain wall and integrated optimization of photovoltaic envelope systems. Appl. Energy 229, 1048–1060. https://doi.org/10.1016/j.apenergy.2018.08.095.
ISO, 2009. International Standard Iso 2009.
Jordan, D.C., Kurtz, S.R., 2013. Photovoltaic degradation rates - an analytical review. Prog. Photovolt. Res. Appl. 21, 12–29. https://doi.org/10.1002/pip.1182.
Karthick, A., Kalidasa Murugavel, K., Kalaivani, L., 2018. Performance analysis of semi-transparent photovoltaic module for skylights. Energy 162, 798–812. https://doi.org/10.1016/j.energy.2018.08.043.
Lee, T.D., Ebong, A.U., 2017. A review of thin film solar cell technologies and challenges. Renew. Sustain. Energy Rev. 70, 1286–1297. https://doi.org/10.1016/j.rser.2016.12.028.
Mehmood, U., Al-Ahmed, A., Al-Sulaiman, F.A., Malik, M.I., Shehzad, F., Khan, A.U.H., 2017. Effect of temperature on the photovoltaic performance and stability of solid-state dye-sensitized solar cells: a review. Renew. Sustain. Energy Rev. 79, 946–959. https://doi.org/10.1016/j.rser.2017.05.114.
Memon, S., Farukh, F., Eames, P.C., Silberschmidt, V.V., 2015. A new low-temperature hermetic composite edge seal for the fabrication of triple vacuum glazing. Vacuum 120, 73–82. https://doi.org/10.1016/j.vacuum.2015.06.024.
Park, K.E., Kang, G.H., Kim, H.I., Yu, G.J., Kim, J.T., 2010. Analysis of thermal and electrical performance of semi-transparent photovoltaic (PV) module. Energy 35, 2681–2687. https://doi.org/10.1016/j.energy.2009.07.019.
Peng, C., Huang, Y., Wu, Z., 2011. Building-integrated photovoltaics (BIPV) in architectural design in China. Energy Build. 43, 3592–3598. https://doi.org/10.1016/j.enbuild.2011.09.032.
Peng, J., Curcija, D.C., Lu, L., Selkowitz, S.E., Yang, H., Zhang, W., 2016. Numerical investigation of the energy saving potential of a semi-transparent photovoltaic double-skin facade in a cool-summer Mediterranean climate. Appl. Energy 165, 345–356. https://doi.org/10.1016/j.apenergy.2015.12.074.
Peng, J., Lu, L., Yang, H., Ma, T., 2015. Comparative study of the thermal and power performances of a semi-transparent photovoltaic façade under different ventilation modes. Appl. Energy 138, 572–583. https://doi.org/10.1016/j.apenergy.2014.10.003.
Pourshaghaghy, A., Omidvari, M., 2012. Examination of thermal comfort in a hospital using PMV-PPD model. Appl. Ergon. 43, 1089–1095. https://doi.org/10.1016/j.apergo.2012.03.010.
Qiu, C., Yang, H., Zhang, W., 2019. Title: Investigation on the energy performance of a novel BIPV system integrated with vacuum glazing. Build. Simul. 29–39.
Ritzen, M.J., Vroon, Z.A.E.P., Rovers, R., Geurts, C.P.W., 2017. Comparative performance assessment of a non-ventilated and ventilated BIPV rooftop configurations in the Netherlands. Sol. Energy 146, 389–400. https://doi.org/10.1016/j.solener.2017.02.042.
Riverola, A., Mellor, A., Alvarez, D.A., Llin, L.F., Guarracino, I., Markides, C.N., 2018. Solar energy materials and solar cells mid-infrared emissivity of crystalline silicon solar cells. Sol. Energy Mater. Sol. Cells 174, 607–615. https://doi.org/10.1016/j.solmat.2017.10.002.
Saretta, E., Caputo, P., Frontini, F., 2019. A review study about energy renovation of building facades with BIPV in urban environment. Sustain. Cities Soc. 44, 343–355. https://doi.org/10.1016/j.scs.2018.10.002.
Selvaraj, P., Ghosh, A., Mallick, T.K., Sundaram, S., 2019. Investigation of semi-transparent dye-sensitized solar cells for fenestration integration. Renew. Energy 141, 516–525. https://doi.org/10.1016/j.renene.2019.03.146.
Shahzad, S., Brennan, J., Theodossopoulos, D., Calautit, J.K., 2018. Does a neutral thermal sensation determine thermal comfort ? Build. Serv. Eng. Res. Technol. https://doi.org/10.1177/0143624418754498.
Shukla, A.K., Sudhakar, K., Baredar, P., Mamat, R., 2018. BIPV based sustainable building in South Asian countries. Sol. Energy 170, 1162–1170. https://doi.org/10.1016/j.solener.2018.06.026.
Singh, M.C., Garg, S.N., Jha, R., 2008. Different glazing systems and their impact on human thermal comfort-Indian scenario. Build. Environ. 43, 1596–1602. https://doi.org/10.1016/j.buildenv.2007.10.004.
Skoplaki, E., Palyvos, J.A., 2009. On the temperature dependence of photovoltaic module electrical performance: a review of efficiency/power correlations. Sol. Energy 83, 614–624. https://doi.org/10.1016/j.solener.2008.10.008.
Sun, Y., Shanks, K., Baig, H., Zhang, W., Hao, X., Li, Y., He, B., Wilson, R., Liu, H., Sundaram, S., Zhang, J., Xie, L., Mallick, T., Wu, Y., 2018. Integrated CdTe PV glazing into windows: energy and daylight performance for different architecture designs. Appl. Energy 231, 972–984. https://doi.org/10.1016/j.apenergy.2018.09.133.
Taffesse, F., Verma, A., Singh, S., Tiwari, G.N., 2016. Periodic modeling of semi-transparent photovoltaic thermal-trombe wall (SPVT-TW). Sol. Energy 135, 265–273. https://doi.org/10.1016/j.solener.2016.05.044.
Thapa, S., Kr, A., Kr, G., 2018. Thermal comfort in naturally ventilated office buildings in cold and cloudy climate of Darjeeling, India – an adaptive approach. Energy Build. 160, 44–60. https://doi.org/10.1016/j.enbuild.2017.12.026.
Traverse, C.J., Pandey, R., Barr, M.C., Lunt, R.R., 2017. Emergence of highly transparent photovoltaics for distributed applications. Nat. Energy 2, 849–860. https://doi.org/10.1038/s41560-017-0016-9.
Wang, M., Peng, J., Li, N., Yang, H., Wang, C., Li, X., Lu, T., 2017. Comparison of energy performance between PV double skin facades and PV insulating glass units. Appl. Energy 194, 148–160. https://doi.org/10.1016/j.apenergy.2017.03.019.
Wang, Z., de Dear, R., Luo, M., Lin, B., He, Y., Ghahramani, A., Zhu, Y., 2018. Individual difference in thermal comfort: a literature review. Build. Environ. 138, 181–193. https://doi.org/10.1016/j.buildenv.2018.04.040.
Young, C.-H., Chen, Y.-L., Chen, P.-C., 2014. Heat insulation solar glass and application on energy efficiency buildings. Energy Build. 78, 66–78. https://doi.org/10.1016/j.enbuild.2014.04.012.
Zhang, W., Lu, L., Peng, J., Song, A., 2016. Comparison of the overall energy performance of semi-transparent photovoltaic windows and common energy-efficient windows in Hong Kong. Energy Build. 128, 511–518. https://doi.org/10.1016/j.enbuild.2016.07.016.
Zhao, J., Luo, S., Zhang, X., Xu, W., 2013. Preparation of a transparent supporting spacer array for vacuum glazing. Vacuum 93, 60–64. https://doi.org/10.1016/j.vacuum.2013.01.002.